

# Precipitated phases and thermodynamic analysis during solidification of Al-Fe-X system at slow cooling rate<sup>①</sup>

TAN Durrqiang(谭敦强), LI Wenxian(黎文献), XIAO Yunde(肖于德), WANG Chong(王冲)  
(School of Materials Science and Engineering, Central South University, Changsha 410083, China)

**Abstract:** The solidification curves of Al-8.5Fe, Al-8.5Fe-1.7Fe, Al-8.5Fe-1.7Si-1.3V alloys were examined by DTA under the condition of slow cooling rate, the phase constituents were examined by OM and XRD. The results show that, under slow cooling rate, the phases in Al-8.5Fe alloy are mainly  $\alpha$ (Al) and Al<sub>13</sub>Fe<sub>4</sub>, the phases in Al-8.5Fe-1.7Si alloy are mostly  $\alpha$ (Al), Al<sub>13</sub>Fe<sub>4</sub>,  $\alpha$ -AlFeSi,  $\beta$ -AlFeSi, and comparing to Al-8.5Fe-1.7Si alloy, no other phases form in the Al-8.5Fe-1.3V-1.7Si alloy, but the chemical compositions of the phases are changed and the thermal stability of  $\alpha$ -AlFeSi phase and  $\beta$ -AlFeSi phase is improved, due to the partial substitution of V for Fe atoms. The phase formation was calculated by Thermo-calc software at equilibrium condition, the calculated results were agreement with the experimental results.

**Key words:** solidification curve; thermodynamic analysis; heat-resistant Al alloy

**CLC number:** TG 132.3

**Document code:** A

## 1 INTRODUCTION

It is an important characteristics that there are lots of excellent thermal stable phases in rapid solidified heat resistant Al alloys<sup>[1-6]</sup>. Strengthening phases in these alloys must have good stabilization of structure and heat-resistance. In the heat resistant Al alloys, there is mutual interaction between the alloy elements and Al matrix, which yields different effects on the microstructures and properties. Generally, some adding elements with low diffusion coefficient and limited solid solution in the aluminium can form intermetallic compounds with high heat-resistance, and aid to improving heat-resistance of Al alloys. When designing these alloys, it is a complex and difficult work to choose theoretically suitable phases with excellent heat-resistance. In fact, we often analyze qualitatively by means of equilibrium thermodynamic theory, and add Ti, V, Cr, Fe, Mo, Zr, Co, Ni, Nb, etc into Al alloys experimentally, so as to obtain some excellent heat-resistant phases, and to prepare heat-resist Al alloys with high stabilities<sup>[7-11]</sup>.

In this paper, the purpose is to analyze structures and constituents of second phases in Al-8.5Fe, Al-8.5Fe-1.7Si, Al-8.5Fe-1.7Si-1.3V alloys prepared at slow cooling rates, and their solidification curves calculated by Thermo-calc software. As a basic research, it will assist with improving microstructures and mechanical properties of rapidly solidified heat-resistant Al alloys.

## 2 THEORETICAL CONSIDERATION

In the ternary Al-Fe-Si system, the liquid, FCC (Al), BCC-A2(Fe), diamond(Si) phases are treated as substitution solutions, with the Gibbs energy expressed as<sup>[12]</sup>:

$$G_m^\Phi = x_{Al}^0 G_{Al}^\Phi + x_{Fe}^0 G_{Fe}^\Phi + x_{Si}^0 G_{Si}^\Phi + RT(x_{Al} \ln x_{Al} + x_{Fe} \ln x_{Fe} + x_{Si} \ln x_{Si}) + G_m^{\Phi} - \Delta^{mg} G_m^\Phi \quad (1)$$

where  $^0 G_i^\Phi$  is the molar Gibbs energy of the element  $i$  ( $i = Al, Fe, Si$ ) with the structure  $\Phi$  in a nonmagnetic state. The term  $^{xs} G_m^\Phi$  is the excess Gibbs energy, expressed in Redlich-Kister polynomial,

$$G_m^{\Phi} = x_{Al} x_{Fe} \sum_{j=0}^n L_{Al, Fe}^{\Phi} (x_{Al} - x_{Fe})^j + x_{Al} x_{Si} \sum_{j=0}^n L_{Al, Si}^{\Phi} (x_{Al} - x_{Si})^j + x_{Si} x_{Fe} \sum_{j=0}^n L_{Fe, Si}^{\Phi} (x_{Fe} - x_{Si})^j + x_{Al} x_{Fe} x_{Si} L_{Al, Fe, Si}^{\Phi} \quad (2)$$

where  $^j L_{Al, Fe}^{\Phi}$ ,  $^j L_{Al, Si}^{\Phi}$ ,  $^j L_{Fe, Si}^{\Phi}$  are the binary interaction parameters taken from the constituent binary systems, and  $L_{Al, Fe, Si}^{\Phi}$  is a ternary interaction parameter with the following form:

$$L_{Al, Fe, Si}^{\Phi} = x_{Al}^0 L_{Al, Fe, Si}^{\Phi} + x_{Fe}^1 L_{Al, Fe, Si}^{\Phi} + x_{Si}^2 L_{Al, Fe, Si}^{\Phi} \quad (3)$$

where  $^j L_{Al, Fe, Si}^{\Phi} = a + bT$ , and  $a$  and  $b$  are model parameters to be evaluated from experimental information.

① **Foundation item:** Project(G1999064900) supported by the National Key Fundamental Research and Development Program of China

**Received date:** 2002-12-11; **Accepted date:** 2003-04-01

**Correspondence:** TAN Durrqiang, Candidate for PhD; Tel: + 86-731-8830261; E-mail: tdunqiang@sohu.com

Fe exhibits antiferromagnetic ordering in the FCC phase and ferromagnetic ordering in the BCC-A2 phase. The magnetic contribution to the Gibbs energy  $\Delta^{\text{mg}} G_m^\Phi$  is described by the expression:

$$\Delta^{\text{mg}} G_m^\Phi = RT \ln(\beta + 1) f(\tau) \quad (4)$$

where  $\tau = T/T_c$ ,  $T_c$  is the critical temperature for magnetic ordering, i.e. the Neel temperature ( $T_N$ ) for antiferromagnetic ordering in the FCC phase, and the Curie temperature ( $T_c$ ) for ferromagnetic ordering in the BCC-A2 phase;  $\beta$  is a quantity related to the total magnetic entropy and, in most cases, is equal to the Bohr magnetic moment per mole of atoms. The term  $f(\tau)$  represents a polynomial obtained by Hillert and Jarl.

There are four stable intermetallic compounds in the Al-Fe system, i.e.  $\text{Al}_5\text{Fe}_2$ ,  $\text{Al}_2\text{Fe}$ ,  $\text{Al}_3\text{Fe}_4$  and  $\theta$ . They are modeled using so-called compound energy model. There is no intermetallic compound in the Al-Si system. The compounds  $\text{Al}_5\text{Fe}_4$  and  $\theta$  are modeled with finite solubility ranges;  $\text{Al}_5\text{Fe}_2$  and  $\text{Al}_2\text{Fe}$  are modeled as stoichiometric phases. In the present work on the Al-Fe-Si system, all binary intermetallic compounds, except  $\theta$ , are treated to have no solubility of the third element due to lack of experimental information. The  $\theta$  phase is treated with a three-sublattice model in the Al-Fe binary system, i.e.  $\text{Al}_{0.6275}\text{Fe}_{0.235}(\text{Al}, \text{Va})_{0.1375}$ , where Va stands for vacancy. In the present work, Si is assumed to dissolve in the third sublattice, i.e.  $\text{Al}_{0.6275}\text{Fe}_{0.235}(\text{Al}, \text{Si}, \text{Va})_{0.1375}$ , since the measured solubility of Si in the compound is within the composition range of this model. Its Gibbs energy function is written as

$$\begin{aligned} G_m^\theta = & y_{\text{Al}}^{\text{III}} G_{\text{Al-Fe-Si}}^\Phi + y_{\text{Si}}^{\text{III}} G_{\text{Al-Fe-Si}}^\Phi + \\ & y_{\text{Va}}^{\text{III}} G_{\text{Al-Fe-Si}}^\Phi + 0.1375 RT (y_{\text{Al}}^{\text{III}} \ln y_{\text{Al}}^{\text{III}} + \\ & y_{\text{Si}}^{\text{III}} \ln y_{\text{Si}}^{\text{III}} + y_{\text{Va}}^{\text{III}} \ln y_{\text{Va}}^{\text{III}}) + \\ & y_{\text{Al}}^{\text{III}} y_{\text{Va}}^{\text{III}} L_{\text{Al-Fe-Al, Va}} + \\ & y_{\text{Al}}^{\text{III}} y_{\text{Si}}^{\text{III}} L_{\text{Al-Fe-Al, Si}} + y_{\text{Si}}^{\text{III}} y_{\text{Va}}^{\text{III}} L_{\text{Al-Fe-Si, Va}} \quad (5) \end{aligned}$$

where  $y_j^{\text{III}}$  stands for the site fraction of  $j$  elements ( $j = \text{Al}, \text{Fe}, \text{Si}$ ) in the third sublattice and

$$\begin{aligned} G_{\text{Al-Fe-X}} = & 0.6275^0 G_{\text{Al}}^{\text{fcc}} + 0.235^0 G_{\text{Fe}}^{\text{bcc}} + \\ & 0.1375^0 G_{\text{X}}^\Phi + a + bT \quad (6) \end{aligned}$$

with X being Al, Fe or Va, and  $G_{\text{Va}} = 0$ . The term  $\Phi$  is FCC for Al and diamond for Si. The term  $L_{\text{Al-Fe-}i, j}$  represents the interaction between the elements  $i$  and  $j$  in the third sublattice, expressed in Redlich-Kister polynomials.

In the ternary Al-Fe-Si system, some ternary compounds will be considered (Table 1).  $\alpha$  and  $\beta$  are modeled as semistoichiometric phases,  $\gamma$  and  $\delta$  are modeled as stoichiometric phases. The Gibbs energy expression for any of the stoichiometric compounds is written as:

$$G_{\text{Al-Fe-Si}}^{\text{Al}_x\text{Fe}_y\text{Si}_z} = x^0 G_{\text{Al}}^{\text{FCC}} + y^0 G_{\text{Fe}}^{\text{BCC}} + z^0 G_{\text{Si}}^{\text{dia}} + a + bT \quad (7)$$

and, for any of the semistoichiometric compounds as:

$$\begin{aligned} G_m^{\text{Al}_x\text{Fe}_y\text{Si}_z(\text{Al, Si})_w} = & y_{\text{Al}}^{\text{IV}0} G_{\text{Al-Fe-Si-Al}}^{\text{IV}0} + \\ & y_{\text{Si}}^{\text{IV}0} G_{\text{Al-Fe-Si-Si}}^{\text{IV}0} + \\ & w RT (y_{\text{Al}}^{\text{IV}} \ln y_{\text{Al}}^{\text{IV}} + y_{\text{Si}}^{\text{IV}} \ln y_{\text{Si}}^{\text{IV}}) + \\ & y_{\text{Al}}^{\text{IV}} y_{\text{Si}}^{\text{IV}} L_{\text{Al-Fe-Si-Al, Si}} \quad (8) \end{aligned}$$

where  ${}^0 G_{\text{Al-Fe-Si-Al}}$  and  ${}^0 G_{\text{Al-Fe-Si-Si}}$  are expressed as

$$\begin{aligned} G_{\text{Al-Fe-Si-Al}} = & (x + w)^0 G_{\text{Al}}^{\text{FCC}} + y^0 G_{\text{Fe}}^{\text{BCC}} + \\ & z^0 G_{\text{Si}}^{\text{dia}} + a + bT \quad (9) \end{aligned}$$

$$\begin{aligned} {}^0 G_{\text{Al-Fe-Si-Si}} = & x^0 G_{\text{Al}}^{\text{FCC}} + y^0 G_{\text{Fe}}^{\text{BCC}} + \\ & (z + w)^0 G_{\text{Si}}^{\text{dia}} + a + bT \quad (10) \end{aligned}$$

and  $L_{\text{Al-Fe-Si-Al, Si}}$  represents the interaction between Al and Si in the fourth sublattice, expressed in Redlich-Kister polynomials.

**Table 1** Ternary intermetallic compounds in Al-Fe-Si system

Name	Model	Crystal structure
$\alpha$	$\text{Al}_{0.66}\text{Fe}_{0.19}\text{Si}_{0.05}(\text{Al, Si})_{0.10}$	Hexagonal
$\beta$	$\text{Al}_{0.598}\text{Fe}_{0.152}\text{Si}_{0.10}(\text{Al, Si})_{0.15}$	Monoclinic
$\gamma$	$\text{Al}_{0.635}\text{Fe}_{0.205}\text{Si}_{0.16}$	Monoclinic
$\delta$	$\text{Al}_{0.49}\text{Fe}_{0.16}\text{Si}_{0.35}$	Tetragonal

### 3 EXPERIMENTAL

Master alloys of Al-8.5% Fe, Al-8.5% Fe-1.7% Si, Al-8.5% Fe-1.7% Si-1.3% V (mass fraction%) were prepared with pure aluminum (99.99%), pure iron (99.99%), pure silicon (99.99%), and Fe-50% V alloy.

DTA curves of the Al-Fe, Al-Fe-Si, Al-Fe-V-Si alloys were examined by TAS100 under continuous cooling regime from 1 000 °C to room temperature at cooling rate of 20 K/min. The second phases are identified in an XD98X X-Ray diffractionmeter with monochromatic  $\text{CuK}_\alpha$  radiation (mean wavelength being 1.5405 Å) over a  $2\theta$  angle range of 20°–80° at a step of 0.03°.

### 4 RESULTS AND DISCUSSION

#### 4.1 Calculated solidification curves

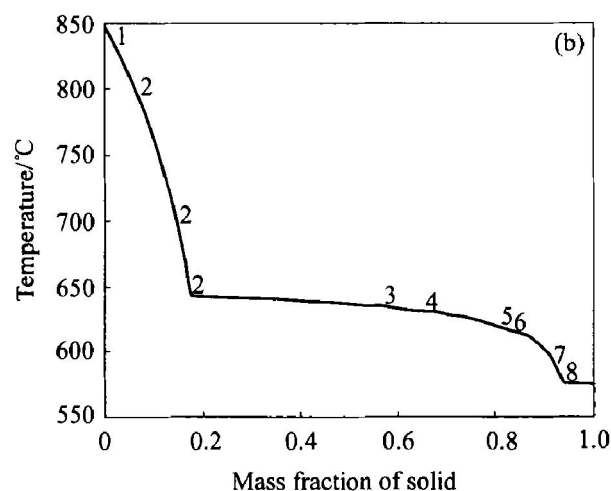
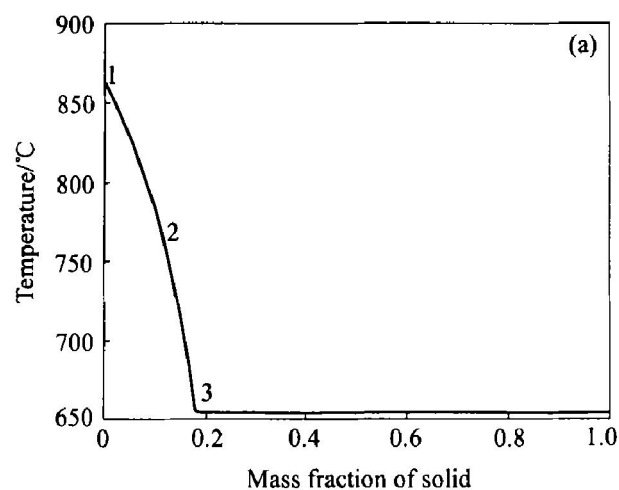
The solidification curves of Al-Fe and Al-Fe-Si alloys were calculated by those models in Thermocalc software, as shown in Fig. 1. In Al-8.5Fe alloy, there are two phases,  $\text{Al}_{13}\text{Fe}_4$  and  $\alpha(\text{Al})$ . In Al-8.5Fe-1.7Si alloy, there are  $\alpha(\text{Al})$ ,  $\text{Al}_{13}\text{Fe}_4$ ,  $\alpha\text{-AlFeSi}$ ,  $\beta\text{-AlFeSi}$  and Si, and the precipitation sequence of the five phases is  $\text{Al}_{13}\text{Fe}_4 \rightarrow \alpha(\text{Al}) \rightarrow \alpha\text{-AlFeSi} \rightarrow \beta\text{-AlFeSi} \rightarrow \text{Si}$ .

#### 4.2 Differential thermal analysis and X-ray diffraction

The characteristic data on the DTA curves of Al-8.5Fe, Al-8.5Fe-1.7Si, Al-8.5Fe-1.3V-1.7Si alloy are summarized in Table 2. XRD patterns of

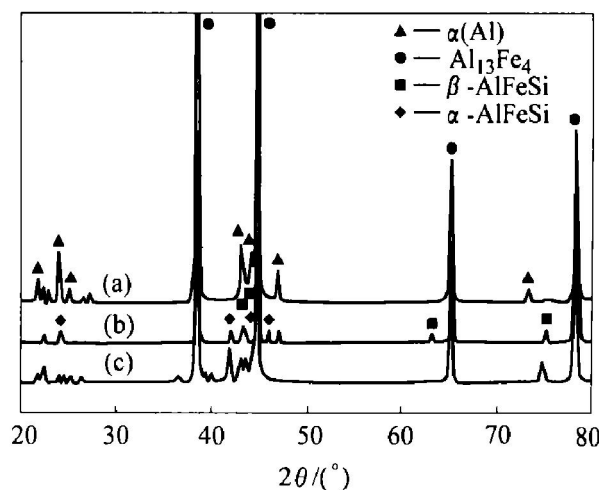
**Table 2** DTA data of Al-Fe system alloys

Alloy	First peak area/ °C			Second peak area/ °C			Third peak area/ °C			Fourth peak area/ °C		
	Begin	Peak	Final	Begin	Peak	Final	Begin	Peak	Final	Begin	Peak	Final
Al-8.5Fe	845	835	700	650	640	620						
Al-8.5Fe-1.7Si	835	823	735	627	623	555	555	550	530	530	527	520
Al-8.5Fe-1.3V-1.7Si	787.5	777	750	647	637	610	610	600	583	583	577	567

**Fig. 1** Solidification curves of Al-8.5Fe and Al-8.5Fe-1.7Si alloys

- (a) —Al-8.5Fe; (b) —Al-8.5Fe-1.7Si  
 1—Liquid; 2—Al<sub>13</sub>Fe<sub>4</sub>, liquid;  
 3—Al<sub>13</sub>Fe<sub>4</sub>, FCC-Al, liquid;  
 4—Al<sub>13</sub>Fe<sub>4</sub>, FCC-Al,  $\alpha$ (Al)FeSi, liquid;  
 5— $\alpha$ -AlFeSi, FCC-Al, liquid;  
 6— $\alpha$ -AlFeSi,  $\beta$ -AlFeSi, FCC-Al, liquid;  
 7— $\beta$ -AlFeSi, FCC-Al, liquid;  
 8— $\beta$ -AlFeSi, diamond-A4, FCC-Al

the three alloys are shown in Fig. 2. In the Al-8.5Fe alloy,  $\alpha$ (Al) and Al<sub>13</sub>Fe<sub>4</sub> equilibrium phase can be detected. In both Al-8.5Fe-1.7Si and Al-8.5Fe-1.3V-1.7Si alloys, there are four kinds of phases. Besides  $\alpha$ (Al) and Al<sub>13</sub>Fe<sub>4</sub> phases, Al<sub>8</sub>Fe<sub>2</sub>Si and Al<sub>3</sub>FeSi equilibrium phases exist in the Al-8.5Fe-1.7Si alloy. Al<sub>8</sub>Fe<sub>2</sub>Si lies in the concentration region of  $\alpha$ -AlFeSi phase while Al<sub>3</sub>FeSi in that of  $\beta$ -AlFeSi.

**Fig. 2** XRD patterns of three alloys  
(a) —Al-Fe; (b) —Al-Fe-Si; (c) —Al-Fe-V-Si

The experimental results match well with the thermodynamics calculation, except that the precipitation temperature is a little lower. But Si phase is not found in Al-8.5Fe-1.7Si, perhaps because its amount is too small. The thermal stabilities of Al<sub>8</sub>Fe<sub>2</sub>Si and Al<sub>3</sub>FeSi are improved by adding V into Al-8.5Fe-1.7Si, without changing the phase structures.

### 4.3 Optical microscopy

OM microstructures of Al-8.5Fe, Al-8.5Fe-1.7Si, Al-8.5Fe-1.3V-1.7Si are shown in Fig. 3. At slow cooling rate, lots of needle-like Al<sub>13</sub>Fe<sub>4</sub> exist in the Al-8.5Fe alloy. Besides needle-like Al<sub>13</sub>Fe<sub>4</sub>, many block particles of  $\alpha$ -AlFeSi phase and needle of  $\beta$ -AlFeSi phases exist in Al-8.5Fe-1.7Si and Al-8.5Fe-1.3V-1.7Si alloys. It is difficult to identify Al<sub>13</sub>Fe<sub>4</sub> and  $\beta$ -AlFeSi from the appearance of phases.

Fortunately, Si is found in the Al-8.5Fe-1.3V-1.7Si sample, as shown in Fig. 4. Generally, Si is easier to dissolve into Al melt than Fe and V, so it is forming during solidification. Perhaps the amount of Si is too small, it can not be detected by X-ray diffractometer.

## 5 CONCLUSIONS

At slow cooling rate, the phases in Al-8.5Fe alloy are mostly  $\alpha$ (Al) and Al<sub>13</sub>Fe<sub>4</sub>, the precipitator

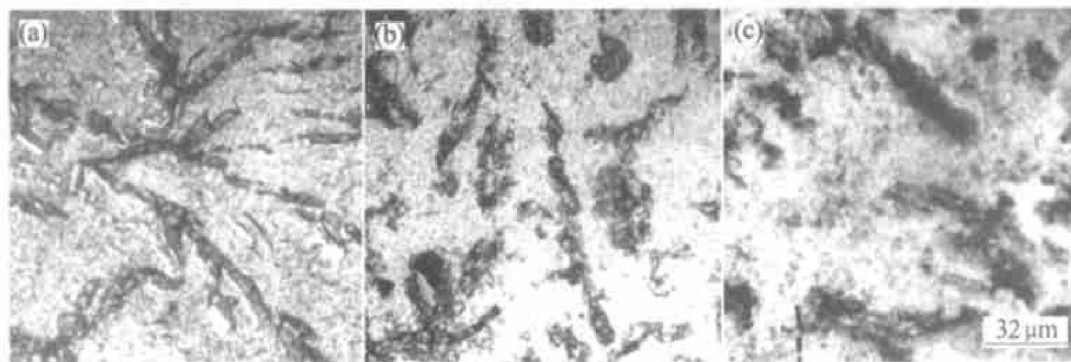


**Fig. 3** Microstructures of three alloys at slow cooling rate  
(a) —Al8.5Fe; (b) —Al8.5Fe-1.7Si; (c) —Al8.5Fe-1.7Si-1.3V

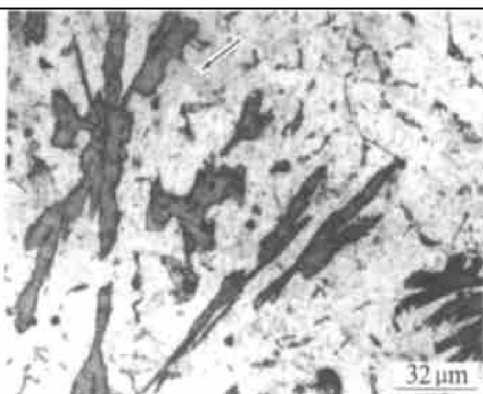


**Fig. 4** Si in Al8.5Fe-1.3V-1.7Si sample  
(at heading of arrow)

on sequence is  $\text{Al}_{13}\text{Fe}_4 \rightarrow \alpha(\text{Al})$ ; in Al8.5Fe-1.7Si alloy, phases are  $\alpha(\text{Al})$ ,  $\text{Al}_{13}\text{Fe}_4$ ,  $\alpha\text{AlFeSi}$  and  $\beta\text{AlFeSi}$ , the sequence is  $\text{Al}_{13}\text{Fe}_4 \rightarrow \alpha\text{Al} \rightarrow \alpha(\text{Al})\text{FeSi} \rightarrow \beta\text{AlFeSi} \rightarrow \text{Si}$ ; in Al8.5Fe-1.3V-1.7Si alloy, comparing to Al8.5Fe-1.7Si alloy, the precipitation sequence and the structure of phases are not changed by adding V, the contents of phases are changed by V substituting some of Fe, increasing the heat-stabilization of  $\alpha\text{AlFeSi}$  and  $\beta\text{AlFeSi}$ .

## REFERENCES

- [1] Dos S K. Rapid solidification and powder metallurgy at Allied-Signal Inc[J]. Inter J Powder Metall, 1986, 24 (2): 175 - 183.
- [2] Singer A R E. Recent developments in the spray forming of metals[J]. Powder Metall, 1985, 21(3): 219 - 225.
- [3] Singer A R E. The challenge of spray forming[J]. Powder Metall, 1982, 25(4): 196 - 203.
- [4] Srivastava A K, Ojha S N, Ranganathan S. Microstructure feature and heat flow analysis of atomized and spray-formed AlFeV-Si alloy[J]. Metall Mater Trans A, 1998, 29(8): 2205 - 2211.
- [5] Das S K, Dasvis L A. High performance aerospace alloys via rapid solidification processing[J]. Mater Sci Eng A, 1988, 98: 1 - 12.
- [6] Griger A, Stefaniay V. Equilibrium and non-equilibrium intermetallic phases in AlFe and AlFe-Si alloys[J]. J Mater Sci, 1996, 31: 6645 - 6652.
- [7] Cochrane P F, Evans P V, Coreer A L. A competitive growth analysis of phase formation in Al8% Fe[J]. Mater Sci Eng A, 1999, 133: 803 - 806.
- [8] Park W J, Ahn S, Kim N J. Effect of cooling rate on the solidification behaviour of AlFe-Si alloys[J]. Mater Sci Eng A, 1994, 189: 291 - 300.
- [9] Skinner D J. The physical metallurgy of dispersion strengthened AlFe-V-Si alloys[J]. Scripta Metall, 1986, 20: 867 - 872.
- [10] Ramanan V R V, Skinner D J. On the nature of icosahedral phase in Al-(Fe, V, Si) alloys[J]. Mater Sci Eng A, 1991, 134: 912 - 920.
- [11] Lee J C, Lee S, Lee D Y. The embrittlement of a rapidly solidified AlFe-V-Si alloy after high-temperature exposure[J]. Metall Mater Trans A, 1991, 22: 853 - 858.
- [12] LIU Zi-kui, Austin Chang Y. Thermodynamic assessment of AlFe-Si system[J]. Metall Mater Trans A, 1999, 30: 1081 - 1095.

(Edited by YUAN Sai-qian)